

Vav Family Rho Guanine Nucleotide Exchange Factors Regulate CD36-mediated Macrophage Foam Cell Formation*

Received for publication, October 7, 2010, and in revised form, December 14, 2010. Published, JBC Papers in Press, January 5, 2011, DOI 10.1074/jbc.M110.192450

S. Ohidar Rahaman^{#1}, Wojciech Swat⁵, Maria Febbraio^{#||2}, and Roy L. Silverstein^{#||2,3}

From the Departments of [†]Cell Biology and [¶]Molecular Cardiology, Cleveland Clinic Lerner Research Institute, Cleveland, Ohio 44195, the ⁵Department of Pathology and Immunology, Washington University School of Medicine, St. Louis, Missouri 63110, and the ^{||}Department of Molecular Medicine, Cleveland Clinic Lerner College of Medicine, Cleveland, Ohio 44195

Lipid-laden macrophages or “foam cells” are the primary components of the fatty streak, the earliest atherosclerotic lesion. Although Vav family guanine nucleotide exchange factors impact processes highly relevant to atherogenesis and are involved in pathways common to scavenger receptor CD36 signaling, their role in CD36-dependent macrophage foam cell formation remains unknown. The goal of the present study was to determine the contribution of Vav proteins to CD36-dependent foam cell formation and to identify the mechanisms by which Vavs participate in the process. We found that CD36 contributes to activation of Vav-1, -2, and -3 in aortae from hyperlipidemic mice and that oxidatively modified LDL (oxLDL) induces activation of macrophage Vav *in vitro* in a CD36 and Src family kinase-dependent manner. CD36-dependent uptake of oxLDL *in vitro* and foam cell formation *in vitro* and *in vivo* was significantly reduced in Vav null macrophages. These studies for the first time link CD36 and Vavs in a signaling pathway required for macrophage foam cell formation.

Atherosclerosis is a complex inflammatory process driven in part by macrophage uptake of oxidized low density lipoproteins (oxLDL)⁴ by scavenger receptors, such as CD36 and scavenger receptor A (1), leading to formation of lipid-laden “foam cells,” the primary component of the earliest atherosclerotic lesions. Studies from our group and others demonstrated that CD36 accounts for a large proportion of foam cell formation *in vitro* and *in vivo* and that interruption of CD36 expression or downstream signaling blocks oxLDL uptake and limits experimental atherosclerosis in mice (2–9). CD36 is a multifunctional, multiligand transmembrane receptor expressed in a diverse array of cells including monocytes/macrophages, platelets, and adipocytes. Interestingly, CD36 deficiency is found in 0.5–1.0% of African and Asian populations (10, 11), and although atherosclerosis has yet to be studied in these groups, monocyte-derived macrophages collected from CD36-null individuals demonstrated 40% less binding and uptake of oxLDL compared with control individuals (12) with significant impairment of

oxLDL-induced activation of NF- κ B and expression of proinflammatory genes (13). Numerous studies have revealed that CD36 acts as a signaling receptor, transmitting signals via Src family kinases (SFK) Lyn and Fyn, and MAP kinases JNK and p38, in response to multiple endogenous and exogenous ligands, including microbial pathogens, oxLDL, apoptotic cells, cell-derived microparticles, thrombospondin-related proteins, and amyloid peptides (14–16). The precise molecular details, however, by which ligation of CD36 leads to recruitment and activation of a signaling complex are not fully understood. Identification of intracellular pathways required for oxLDL uptake and foam cell formation is vital for understanding the initiating stages of atherosclerosis and for designing novel targeted inhibitory agents. The studies outlined here demonstrate a critical role for Vav proteins in mediating CD36-dependent oxLDL uptake and foam cell formation in macrophages.

The three structurally and functionally related members of the Vav family (Vavs) are multidomain signal transduction molecules that act as guanine nucleotide exchange factors for Rac1 and Rho GTPases and also function as adaptor platforms, interacting directly with signaling proteins including dynamin, phospholipase C- γ ; ZAP70, Lyn, and Syk (17, 18). In these capacities Vavs may regulate multiple processes, including NADPH oxidase-mediated generation of reactive oxygen species (19, 20) and fission of endocytic vesicles from the plasma membrane (21, 22). Vav1 is expressed exclusively in hematopoietic cells, whereas Vav2 and Vav3 are widely expressed. Vavs have both unique and overlapping functions and can be activated by several pathways, including ligation of antigen receptors, integrins, growth factor receptors, and chemokine receptors (17, 23–25). In microglial cells Vav1 has been implicated in CD36-mediated responses to fibrillar A β amyloid peptides (21). Because Vav signaling impacts processes highly relevant to atherogenesis and involves pathways common to CD36 signaling, we hypothesized that Vavs could mechanistically link oxLDL-mediated CD36 signaling in macrophages to proatherogenic responses. We now show that CD36 plays an important role *in vivo* and *in vitro* in activation of Vavs during hyperlipidemic conditions via activation of SFKs. Mechanistically we demonstrate that Vavs regulate CD36-mediated macrophage foam cell formation by controlling internalization of oxLDL in cells.

EXPERIMENTAL PROCEDURES

Antibodies, Cells, and Reagents—Antibodies to Vav1 and Vav2 were from Santa Cruz Biotechnology (Santa Cruz, CA).

* This work was supported, in whole or in part, by National Institutes of Health Grant HL087018.

¹ To whom correspondence may be addressed. E-mail: rahamao@ccf.org.

² Both authors contributed equally to this work.

³ To whom correspondence may be addressed. E-mail: silverr2@ccf.org.

⁴ The abbreviations used are: oxLDL, oxidatively modified LDL; apoE, apolipoprotein E; MPM, mouse peritoneal macrophage; SFK, Src family kinase; Dil, 1,1'-Diiododecyl-3,3,3',3'-tetramethylindocarbocyanide iodide.

Anti-Lyn antibody was from BD Transduction, and anti-phosphotyrosine clone 4G10 and anti-Vav3 antibodies were from Upstate Biotechnology. Antibody to inhibit CD36 was purchased from Cayman Chemicals, and CD68 antibody was from AbD Serotec (Oxford, UK). LDL was isolated from fresh human plasma as described previously and stored under N₂ gas until use. All LDL concentrations were expressed in terms of protein content as measured by Lowry assay. Copper-oxidized LDL was prepared by incubating LDL with CuSO₄ (5 μM) for 8 h at 37 °C, and LDL oxidized by the leukocyte myeloperoxidase/nitrite system (NO₂LDL) was prepared as described previously (2). DiI and LY294002 were from Calbiochem. All other chemicals were obtained from Sigma unless indicated.

CD36^{-/-}, apoE^{-/-}CD36^{-/-}, Vav1^{-/-}Vav3^{-/-}, apoE^{-/-} mice were described previously. Vav1^{-/-} mice were provided by Dr. J. Rivera (National Institutes of Health). Mice were backcrossed at least six times to C57BL/6, and background-matched WT control lines were used in all studies. Thioglycollate-elicited peritoneal macrophages were isolated and maintained as described previously (5). THP-1 cells were from American Type Culture Collection. 3T3L1 preadipocytes were differentiated using the adipogenesis kit from Cayman Chemicals. All cell culture reagents were purchased from Invitrogen.

Binding and Uptake of NO₂LDL—Mouse peritoneal macrophages (MPMs) plated on coverslips were incubated with DiI-NO₂LDL (5 μg/ml) for 30 min at 4 °C. Fluorescence intensity was examined by confocal or epifluorescence microscopy. To assess uptake, cells were then warmed to 37 °C and imaged at timed points up to 30 min. CD36^{-/-} cells were used to assess nonspecific binding.

Foam Cell Assays—Thioglycollate-elicited MPMs from various strains were plated on coverslips in 12-well plates in RPMI 1640 medium supplied with 10% FCS. After 2 h, nonadherent cells were removed, and fresh medium was added for 48 h. Cells were then incubated with 50 μg/ml native or modified LDL for 8 h. Cells were fixed with 4% formaldehyde and stained with Oil Red O, and foam cells were counted by microscopy. For inhibition of CD36-mediated foam cell formation in Vav1^{-/-} MPMs, cells were preincubated with anti-CD36 IgG or control IgG (10 μg/ml) for 4 h then continued for an additional 8-h incubation in presence of NO₂LDL. For the *in vivo* assays, elicited MPMs were collected from male donor mice of various genotypes, and 10⁷ cells were then injected intraperitoneally into each recipient apoE^{-/-} mouse maintained on a diet containing 0.15% cholesterol and 42% milk fat (TD88137; Harlan-Teklad) for 6 weeks. After 3 days, recipient mice were lavaged and cells analyzed as above by Oil Red O staining.

Immunoprecipitation and Immunoblot Analysis—For IP studies, tissues or cells from mice were lysed in 20 mM Tris-HCl (pH 7.5), 150 mM NaCl, 1 mM EDTA, 1 mM EGTA, 1% Nonidet P-40, 2.5 mM sodium pyrophosphate, 1 mM β-glycerophosphate, 1 mM Na₃VO₄, and 1 μg/ml leupeptide. The cleared supernatant containing 300–500 μg of protein was incubated with 2–3 μg of antibody immobilized on agarose beads overnight at 4 °C. Beads were washed extensively in the same buffer and then boiled in SDS-PAGE loading buffer for subsequent immunoblotting. Immunoblots were analyzed with a chemiluminescence detection system.

RESULTS

CD36-dependent Activation of Vav by Hyperlipidemia and Oxidized Phospholipids—To understand the role of Vavs in CD36-dependent foam cell formation, we first examined the activation status of Vav proteins *in vivo* using apoE^{-/-} and apoE^{-/-}CD36^{-/-} mice maintained on a Western diet for 12 weeks to induce hyperlipidemia (5). Vav proteins were immunoprecipitated from aorta and fat tissue lysates with specific antibodies to the three Vav family members, and the immunoprecipitates were then probed by immunoblotting with an anti-phosphotyrosine (anti-(Tyr(P))) monoclonal IgG because both the catalytic and adaptor activity of Vavs are dependent on tyrosine phosphorylation (17). Fig. 1A shows increased phosphorylation of all three Vavs in aorta and fat in apoE^{-/-} mice compared with apoE^{-/-}CD36^{-/-}. The -fold increases were 3.7, 10.6, and 4.2, respectively, for Vav-1, -2, and 3 in aorta and 5.0, 2.5, and 3.6 in fat. Immunoblots with antibody to CD68, a specific marker for tissue macrophages (Fig. 1A, lower panel) showed equal amount of CD68 antigen in aorta and fat tissues from apoE^{-/-} and apoE^{-/-}CD36^{-/-} mice, suggesting that the differences in Vav phosphorylation were not due to differences in tissue macrophage content in the different genotypes. Mice fed a chow diet showed less Vav phosphorylation than high fat diet-fed animals, and no significant differences were observed between apoE^{-/-} and apoE^{-/-}CD36^{-/-} mice (Fig. 1B).

To examine Vav activation under more defined *in vitro* conditions, MPMs were treated with copper-oxidized LDL (Cu²⁺-oxLDL) or NO₂LDL, a form of oxLDL that is highly specific for CD36 (2) for timed periods from 2 to 30 min. Fig. 2A shows a representative blot for Vav1 demonstrating significantly increased phosphorylation induced by both forms of oxLDL ($p < 0.01$) compared with the untreated control cells shown at 0 min. The bar graphs in Fig. 2B show the mean increases in Vav1 (top) and Vav3 (bottom) phosphorylation at each time point after treatment with Cu²⁺-oxLDL (left panels) or NO₂LDL (right panels). Cells treated with native LDL did not show any increase in Vav1 or Vav3 phosphorylation over the 30-min period (data not shown). Human THP-1 monocytic cells were also studied, and a 1.8-fold increase in phosphorylation of Vav1 was seen at 30 min in response to Cu²⁺-oxLDL compared with native LDL (Fig. 2C; *, $p < 0.05$). The different Vav1 activation kinetics in THP-1 cells compared with MPMs (30 min versus 2 min) could be due to differences in recruitment and activation of specific SFKs by oxLDL/CD36 engagement in human versus mouse cells or in a transformed monocytic cell line versus differentiated tissue macrophages. No significant activation of Vav2 or Vav3 was detected in the human cells (data not shown). To strengthen the observation that Vavs are activated in a CD36-dependent manner, we also compared Vav1 and Vav3 activation in WT and CD36^{-/-} MPMs. Fig. 2D shows representative blots and corresponding bar graphs for Vav1 and Vav3 phosphorylation, demonstrating significantly increased phosphorylation of both Vavs in WT compared with CD36^{-/-} MPMs. Isotype-matched control IgGs were used to show specificity of the anti-Vav antibodies (Fig. 2E), and all blots were stripped and reprobed with anti-Vav antibodies to control for protein loading. Together, these results show that in

Vav Signaling in Hyperlipidemic Conditions

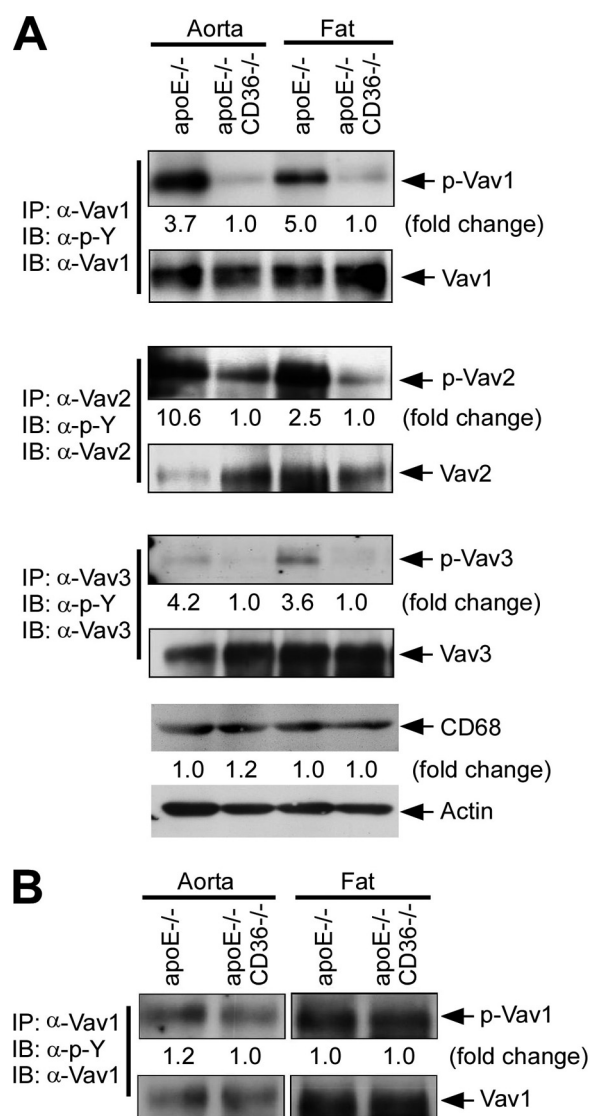


FIGURE 1. Hyperlipidemic conditions induce CD36-dependent activation of Vav-family members *in vivo*. Extracts from aorta and fat obtained from apoE^{-/-} or apoE^{-/-}CD36^{-/-} mice maintained on Western (A) or normal chow (B) diets for 12 weeks were immunoprecipitated (IP) with antibodies to the three specific Vav family members. Precipitates were then subjected to immunoblotting (IB) with anti-Tyr(P), and the blots then stripped and reprobed with antibodies to the individual Vavs to assess total protein loaded. Blots were scanned to quantify band densities and normalized to the respective total protein loads. The -fold change comparing single-null to double-null mice is indicated below each blot. To assess macrophage content, lysates from aorta and fat tissues were also probed with anti-CD68 antibody (lower panel). As a loading control and for normalization, blots were also probed for actin. Blots from normal chow diets are shown separately because of higher exposure times compared with blots shown in A due to less activation of p-Vav1. Blots were quantified and normalized to the respective total protein loads. Pooled extracts from at least three mice were used for each study.

atherogenic conditions Vavs are activated both *in vivo* and *in vitro* in a CD36-dependent fashion.

During hyperlipidemic conditions aorta and fat tissues are infiltrated by hematopoietic cells with abundant macrophages present. Vav1 is expressed only in hematopoietic cells whereas Vav2 and Vav3 are ubiquitously present in most of the cell types. Therefore, it is reasonable to conclude that the Vav1 activation seen in aorta and fat (Fig. 1A) in advanced atheroma is due in part to the presence of infiltrating hematopoietic cells

(most likely macrophages). Hematopoietic cells, adipocytes, smooth muscle cells, and possibly other cell types may contribute to the phosphorylated Vav2 and Vav3 seen *in vivo*. To address these issues we examined Vav2 and Vav3 activation in adipocytes by NO₂LDL. Fig. 2E demonstrates increased phosphorylation of Vav2 (5-fold at 30 min) and Vav3 (3-fold at 5 min) compared with untreated control adipocytes differentiated from 3T3L1 cells.

CD36-mediated Vav Activation Is Regulated by SFKs—We recently showed that oxLDL-CD36 engagement on macrophages led to recruitment of a signaling complex containing Lyn and the upstream MAP kinase kinase MEKK2 that led to activation of JNK (9). To determine whether SFK activation is upstream of Vav activation by oxLDL, MPMs were first treated with a broadly active SFK inhibitor (PP2) prior to exposure to NO₂LDL. Immunoprecipitation/immunoblot analyses revealed that activation of Vav1 and Vav2 was nearly completely abrogated in the presence of the SFK inhibitor (Fig. 3A), whereas no inhibition was observed in presence of an unrelated kinase inhibitor, LY. To determine the role of Lyn in this system, specific immunoprecipitations of the three Vavs were done from oxLDL-treated MPMs and from aorta and fat tissue lysates from high fat diet-fed mice. Immunoprecipitates were then probed by immunoblotting with anti-Lyn IgG, demonstrating an interaction of Vavs with Lyn in cells (Fig. 3B). To show the specificity of Vav1 interaction with Lyn, we performed immunoprecipitation/immunoblotting using isotype-matched control IgG (Fig. 3B, bottom panel). To validate the Vav-Lyn interaction, we also performed reciprocal immunoprecipitation. Fig. 3C shows that anti-Lyn IgG precipitated all three Vav proteins, confirming the results shown in Fig. 3B. No increased interactions were seen comparing oxLDL-treated cells with PP2-treated or control cells, suggesting that the Vav-Lyn interaction is constitutive; that is, not dependent on ligand engagement or Lyn or Vav activation. Lyn also co-precipitated with all three Vavs from aorta and fat, but substantially more Lyn appeared to be associated with Vavs in apo^{-/-} compared with apoE^{-/-}CD36^{-/-} tissues (2.1-, 6.2-, and 2.7-fold increases, respectively, in Vav1, Vav2, and Vav3 in aorta and 3.0-, 1.2-, and 1.7-fold, respectively, increases in fat) (Fig. 4). These results suggest that Vav activation is regulated by SFKs and CD36 facilitates interaction of Vav proteins with Lyn in hyperlipidemic conditions.

Vavs Are Required for CD36-dependent Macrophage Foam Cell Formation—To examine the *in vivo* role of Vavs in macrophage foam cell formation, we used an *in vivo* foam cell assay developed by Li *et al.* involving macrophage transfer from genetically defined donors into the peritoneal cavities of hyperlipidemic, Western diet-fed apoE^{-/-} recipients (26). After 72 h, cells were lavaged from the peritoneal cavities and foam cells quantified by Oil Red O staining. Fig. 5A shows that ~73% of WT donor macrophages stained with Oil Red O, indicating foam cell formation, whereas only 16% of those from Vav1^{-/-}Vav3^{-/-} donors took up the stain. To examine foam cell formation under more defined *in vitro* conditions, MPMs from genetically altered mice were treated with NO₂LDL, and foam cell formation was quantified by Oil Red O staining. CD36-dependent *in vitro* macrophage foam cell for-

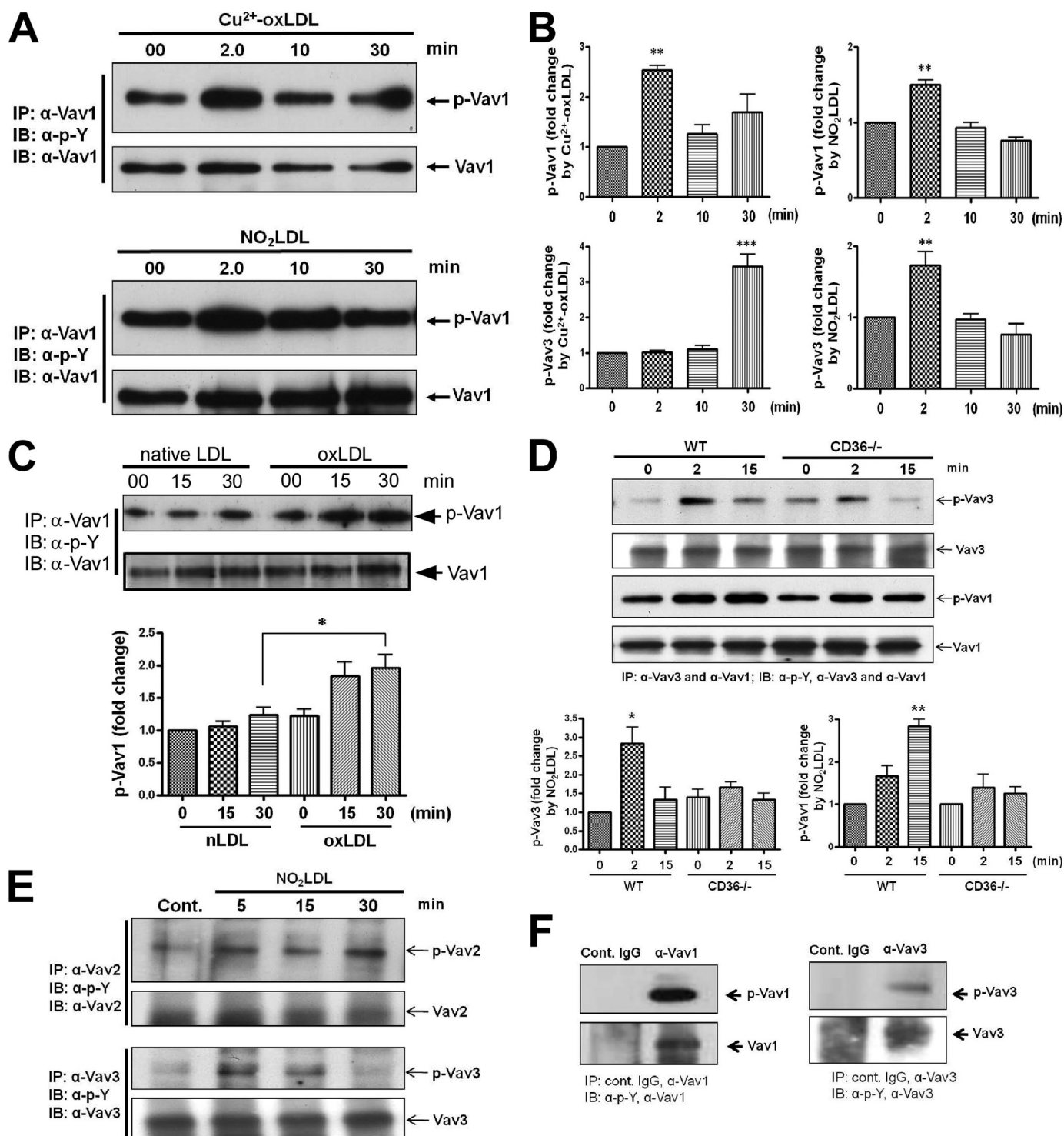


FIGURE 2. OxLDL induces CD36-dependent activation of Vav family members *in vitro*. *A*, representative *in vitro* study shows MPMs exposed to Cu²⁺-oxLDL or NO₂LDL (50 μg/ml) for timed periods to 30 min and Vav activation assessed as above by immunoprecipitation (IP)/immunoblotting (IB). *B*, blots as in *A* from at least three separate experiments were scanned, and -fold changes in band densities of phosphorylated Vav1 (top panels) and Vav3 (bottom panels) were plotted after normalization to the respective total protein loads. Error bars indicate S.D., and asterisks indicate statistical significance determined by one-way ANOVA. *C*, human THP-1 monocytic cells exposed to native or oxLDL for timed periods were analyzed as in *A* for Vav1 phosphorylation. Blots from three separate experiments were scanned to quantify band densities and normalized to the respective total protein loads. Error bars indicate S.D., and asterisks indicate statistical significance determined by one-way ANOVA. *D*, representative *in vitro* study shows MPMs from WT and CD36^{-/-} mice exposed to NO₂LDL (50 μg/ml) for timed periods to 15 min and Vav activation assessed as above by immunoprecipitation/immunoblotting. Blots from three separate experiments were scanned, and -fold change in band densities of phosphorylated Vav1 and Vav3 were plotted after normalization to the respective total protein loads. Error bars indicate S.D., and asterisks indicate statistical significance determined by one-way ANOVA. *E* and *F*, adipocytes differentiated from 3T3L1 cells untreated or exposed to NO₂LDL (50 μg/ml) for timed periods were analyzed for Vav2 and Vav3 phosphorylation as described above (*E*). Cell extracts were immunoprecipitated with isotype-matched control IgG or antibodies to either Vav1 or Vav3 to show specificity (*F*). In all studies *, $p < 0.05$; **, $p < 0.01$; and ***, $p < 0.001$.

Vav Signaling in Hyperlipidemic Conditions

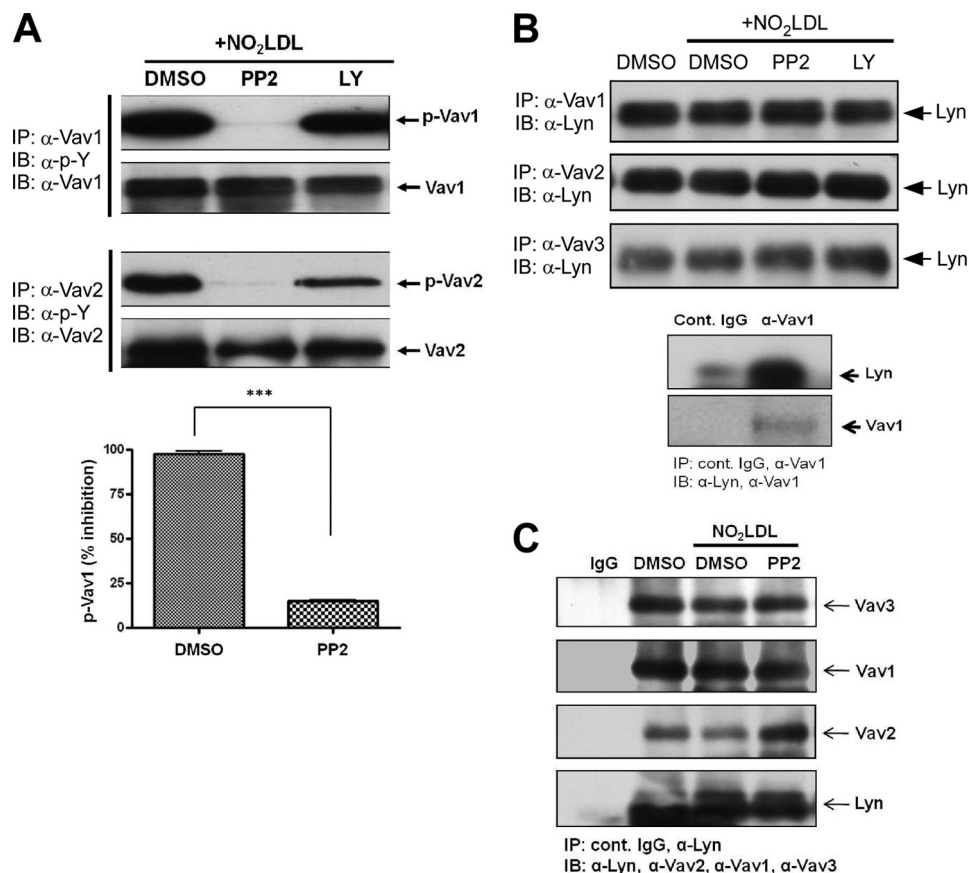


FIGURE 3. Lyn associates with Vav *in vitro* and is necessary for oxLDL-induced Vav activation. *A*, MPMs were stimulated with NO₂LDL (50 μg/ml) for 2 min after preincubation with either vehicle (dimethyl sulfoxide (DMSO)) or a broadly active Src inhibitor (PP2, 10 μM) for 60 min. An inhibitor to PI3Ks (LY, 10 μM) was used as an additional control. *Top panels* shows Vav1 and Vav2 phosphorylation, assessed by immunoprecipitation (IP)/immunoblotting (IB) as in Fig. 1. *Bar graph* of means ± S.E. from three separate experiments shows an 85% decrease in Vav1 phosphorylation in the presence of PP2 (***, *p* < 0.0001, Student's *t* test). *B*, extracts from MPMs treated as in *A* were subjected to immunoprecipitation with anti-Vav antibodies and then probed by immunoblotting with anti-Lyn IgG. Cell extracts were immunoprecipitated with isotype-matched control IgG or antibody to Vav1 to show specificity of its interaction with Lyn (*bottom panel*). *C*, for reverse immunoprecipitation, MPMs were stimulated with NO₂LDL (50 μg/ml) for 2 min after preincubation with either vehicle (dimethyl sulfoxide) or a broadly active Src inhibitor (PP2, 10 μM) for 60 min. Extracts were subjected to immunoprecipitation with anti-Lyn antibody and then probed by immunoblotting with antibodies to Vav proteins and Lyn. Cell extracts were immunoprecipitated with isotype-matched control IgG to show specificity.

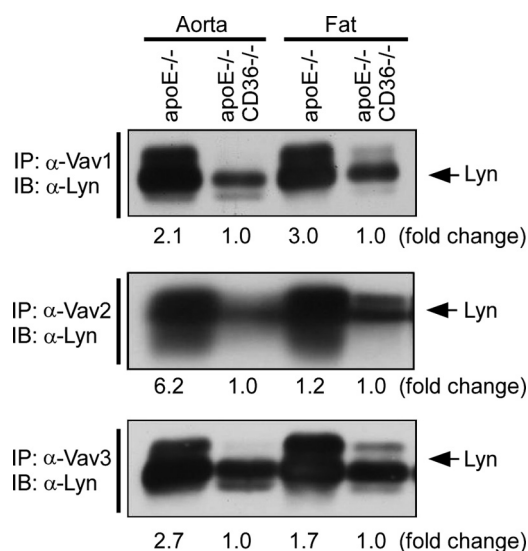


FIGURE 4. CD36 facilitates interaction of Vav proteins with Lyn in hyperlipidemic conditions. Aorta and fat extracts from hyperlipidemic apoE^{-/-} and apoE^{-/-}CD36^{-/-} mice were subjected to immunoprecipitation (IP) with antibodies to the three Vav proteins followed by immunoblotting (IB) with anti-Lyn. Pooled extracts from at least three mice were used for each group. Blots were scanned and quantified as in Fig. 1 comparing single-null to double-null mice.

mation was partially impaired in Vav1-null MPMs (Fig. 5B), whereas Vav1^{-/-}Vav3^{-/-} cells showed a much more severe impairment. To link Vav proteins to CD36-mediated foam cell formation causally, Vav1^{-/-} cells were incubated with anti-CD36 IgG prior to adding NO₂LDL. Fig. 5C shows that ~60% of Vav1^{-/-} macrophages treated with control IgG stained with Oil Red O, indicating foam cell formation, whereas only 25% of cells treated with anti-CD36 IgG took up the stain. Together, these data suggest that Vavs plays critical role during CD36-mediated macrophage foam cell generation.

Vavs Play a Critical Role in CD36-dependent OxLDL Uptake in Macrophages—To probe the mechanism by which Vavs influence CD36-mediated foam cell formation, we examined binding and internalization of oxLDL in macrophages. MPMs from WT and Vav-null mice were incubated with DiI-NO₂LDL at 4 °C followed by 37 °C to assess the role of Vavs in CD36-dependent binding and internalization of oxLDL. No significant differences in binding to Vav1^{-/-} cells compared with WT were observed, but null cells showed significantly less fluorescence accumulation at 30 min compared with WT (Fig. 6, A and B). Because Vav family members have both overlapping and unique functions we also assessed DiI-

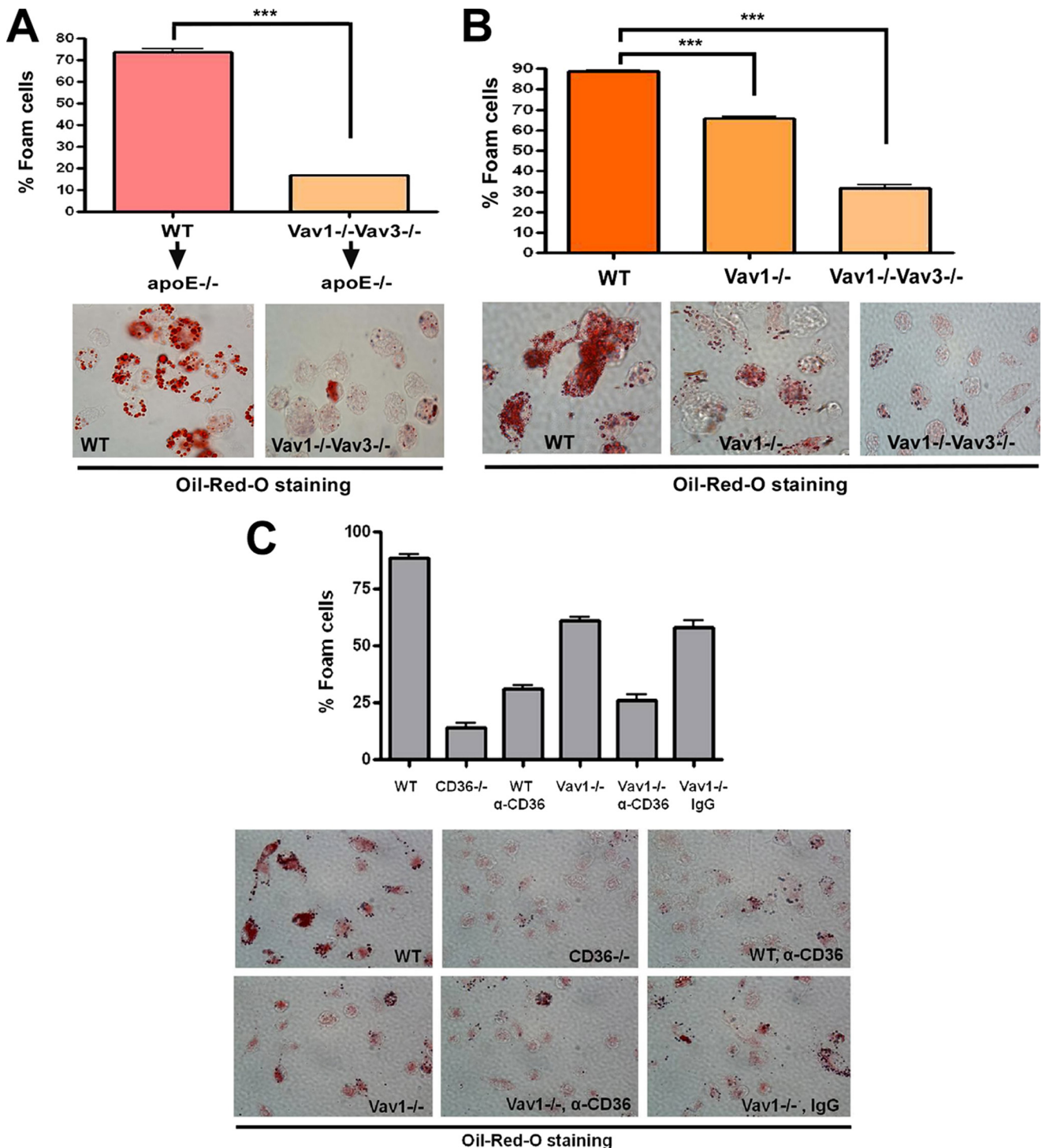


FIGURE 5. CD36-mediated foam cell formation is Vav-dependent. *A*, MPMs were collected from WT and Vav1^{-/-}Vav3^{-/-} mice and injected intraperitoneally into apoE^{-/-} recipient mice ($n = 6$ for each group) that had been maintained on a Western diet for 6 weeks. After 72 h, cells were recovered from the peritoneal cavity and stained with Oil Red O to quantify *in vivo* foam cell formation. *Bar graphs* show means \pm S.E. from four randomly chosen fields from each group (***, $p < 0.0001$, Student's *t* test). *B*, MPMs from WT, Vav1^{-/-}, and Vav1^{-/-}Vav3^{-/-} mice were incubated with NO₂LDL (50 μ g/ml) for 8 h, stained with Oil Red O, and analyzed microscopically to quantify foam cell formation. *Bar graphs* show the means \pm S.E. from four randomly chosen fields from each group (***, $p < 0.0001$, Student's *t* test). *C*, MPMs from WT, Vav1^{-/-}, and CD36^{-/-} mice were incubated with NO₂LDL (50 μ g/ml) for 8 h after preincubation with anti-CD36 or IgG control for 4 h. Cells were stained with Oil Red O and analyzed microscopically to quantify foam cell formation. *Bar graphs* show the means \pm S.E. from four randomly chosen fields from each group.

NO₂LDL binding and uptake in Vav1^{-/-}Vav3^{-/-} cells and found that although binding was not affected, internalization was severely impaired (Fig. 6C). After 30 min, WT cells showed NO₂LDL accumulation in a small number of large perinuclear

vesicles, whereas in the Vav1^{-/-} and Vav1^{-/-}Vav3^{-/-} cells NO₂LDL accumulated in small vesicles mostly on or close to the plasma membrane, suggesting a possible defect in vesicle maturation.

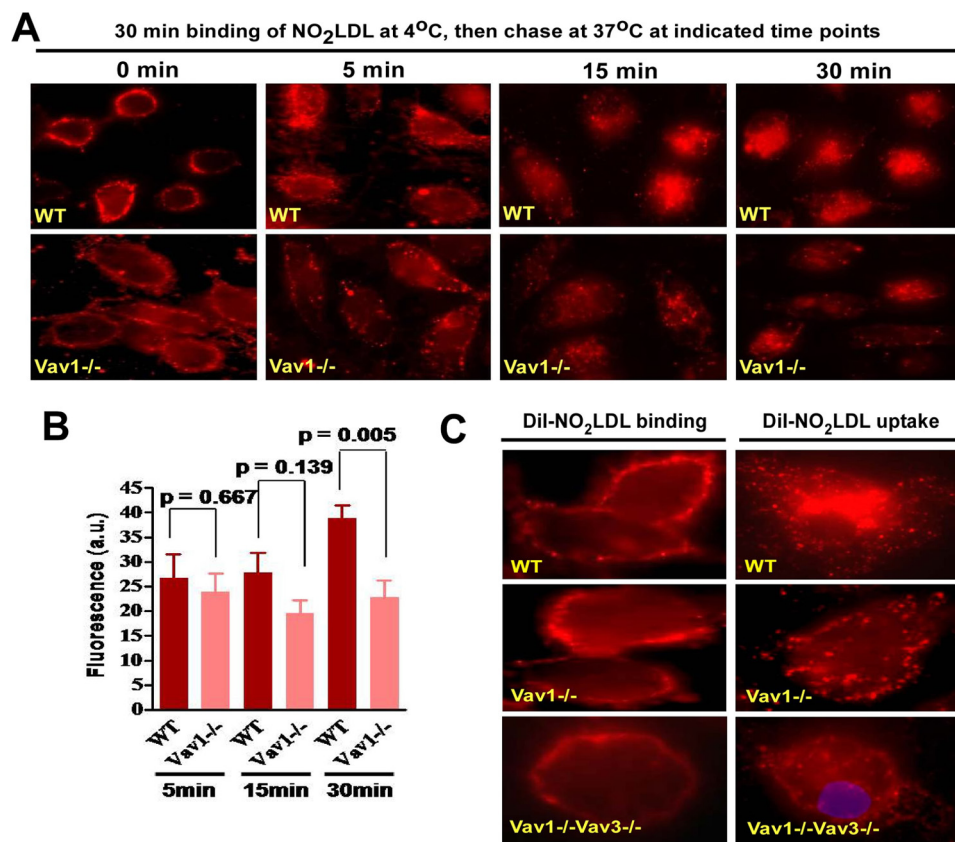


FIGURE 6. **CD36-mediated oxLDL uptake is regulated by Vav proteins.** A, WT and Vav1^{-/-} MPMs were incubated with Dil-labeled NO₂LDL at 4 °C and then transferred to 37 °C to measure uptake. B, bar graph shows mean cellular fluorescence. For quantitation we measured fluorescence intensity of 8–10 randomly selected cells from each group by ImageJ software. Experiments were repeated three or more times, and *p* values were calculated by unpaired Student's *t* test. C, higher power images of MPMs from WT, Vav1^{-/-}, and Vav1^{-/-}Vav3^{-/-} mice were treated as above to show binding and uptake of Dil-labeled NO₂LDL.

DISCUSSION

As part of the innate immune system macrophage CD36 participates in recognition and clearance of exogenous pathogen-derived ligands as well as endogenous modified “self” molecules (14, 15). The latter role, which includes uptake of oxidized lipoproteins, presumably serves a homeostatic function, but in the context of a modern “Western” lifestyle that predisposes to oxidant stress and hyperlipidemia, oxidized phospholipid ligands are abundant, CD36 expression is up-regulated, and CD36 signaling becomes pathological, promoting a proatherogenic response. In this setting CD36-mediated lipid uptake cannot be mitigated by efflux mechanisms, thereby contributing to foam cell formation. Furthermore, activation of CD36-mediated intracellular signaling cascades promotes vascular inflammation and interferes with macrophage migration, leading to their accumulation in the vessel wall (27, 28). Although there has been some controversy about the contribution of CD36 to atherogenesis (29), studies of several murine *in vivo* model systems, including high fat diet-stressed apoE^{-/-} and LDLR^{-/-} strains crossed into at least two CD36^{-/-} strains, as well as studies of CD36^{-/-} bone marrow chimeras and CD36 inhibitor-treated mice have shown dramatically smaller plaque lesions and/or less complex lesions with less aortic cholesterol in the absence of functional CD36 (5–8, 30, 31). Importantly, recent genome-wide association studies in humans suggest a link between CD36 polymorphisms and myocardial infarction, further supporting this hypothesis (32).

Understanding the molecular details of the intracellular processes activated by oxLDL-CD36 engagement is thus an important goal and could lead to identification of novel therapeutic targets for atherothrombotic disorders. CD36 signaling has been studied in several cellular contexts, including microvascular endothelial cell responses to thrombospondins, microglial cell responses to A β amyloid peptides, macrophage and platelet responses to oxidized phospholipids, and neuroepithelial cell responses to fatty acids (14, 15, 33). These studies have revealed a common theme involving recruitment and activation of cell-specific Src family nonreceptor tyrosine kinases with subsequent activation of specific MAP serine/threonine kinases. Our laboratory showed that the C-terminal cytoplasmic domain of CD36 is sufficient for assembling a signaling complex that includes Src family kinases and upstream MAP kinase kinases (9), and others have defined a critical role for two cytoplasmic cysteine residues in mediating CD36 signals (34). We previously reported a central role for Lyn in CD36-mediated macrophage responses to oxLDL and defined a signaling pathway that included activation of the MAP kinase JNK and the tyrosine kinase focal adhesion kinase and inactivation of the phosphatase SHP2 (9, 28). JNK activation was shown to be required for oxLDL internalization and foam cell formation, whereas sustained activation of focal adhesion kinase was shown to contribute to oxLDL inhibition of migration and “fixation” of macrophages at inflammatory sites.

In this paper we now identify an important role for the Vav family of guanine nucleotide exchange factors in mediating CD36 function. We used *in vivo* and *in vitro* models of hyperlipidemia and oxidant stress to show CD36-dependent activation of all three Vavs in a manner that requires Src kinases (most likely Lyn). This is consistent with work from Landreth's group showing that engagement of CD36 on microglial cells by A β peptide induced Vav1 activation (21). Interestingly, whereas deletion of a single Vav (Vav1) led to modest inhibition of oxLDL uptake and foam cell formation, deletion of two Vavs (Vav1 and 3) led to nearly complete loss of foam cell formation (Fig. 5), suggesting overlapping and redundant functions for these proteins. Mechanistically, we demonstrate that impaired maturation of endocytic vesicles carrying oxLDL presumably played a role in disrupted foam cell formation in cells deficient of Vav proteins (Fig. 6C), suggesting that oxLDL may be distributed to endocytic vesicles following a Vav-dependent pathway. These data are consistent with published studies showing critical role of Vav members as regulator of ligand-receptor endocytosis in various cell types (21, 22). Altogether, these studies identified Vav proteins as a critical regulator of oxLDL-CD36 signaling pathway that is important in atherogenesis and thus represent novel targets for therapeutics.

REFERENCES

- Glass, C. K., and Witztum, J. L. (2001) *Cell* **104**, 503–516
- Podrez, E. A., Febbraio, M., Sheibani, N., Schmitt, D., Silverstein, R. L., Hajjar, D. P., Cohen, P. A., Frazier, W. A., Hoff, H. F., and Hazen, S. L. (2000) *J. Clin. Invest.* **105**, 1095–1108
- Podrez, E. A., Poliakov, E., Shen, Z., Zhang, R., Deng, Y., Sun, M., Finton, P. J., Shan, L., Febbraio, M., Hajjar, D. P., Silverstein, R. L., Hoff, H. F., Salomon, R. G., and Hazen, S. L. (2002) *J. Biol. Chem.* **277**, 38517–38523
- Zhao, Z., de Beer, M. C., Cai, L., Asmis, R., de Beer, F. C., de Villiers, W. J., and van der Westhuyzen, D. R. (2005) *Arterioscler. Thromb. Vasc. Biol.* **25**, 168–173
- Febbraio, M., Podrez, E. A., Smith, J. D., Hajjar, D. P., Hazen, S. L., Hoff, H. F., Sharma, K., and Silverstein, R. L. (2000) *J. Clin. Invest.* **105**, 1049–1056
- Febbraio, M., Guy, E., and Silverstein, R. L. (2004) *Arterioscler. Thromb. Vasc. Biol.* **24**, 2333–2338
- Guy, E., Kuchibhotla, S., Silverstein, R., and Febbraio, M. (2007) *Atherosclerosis*. **192**, 123–130
- Kuchibhotla, S., Vanegas, D., Kennedy, D. J., Guy, E., Nimako, G., Morton, R. E., and Febbraio, M. (2008) *Cardiovasc. Res.* **78**, 185–196
- Rahaman, S. O., Lennon, D. J., Febbraio, M., Podrez, E. A., Hazen, S. L., and Silverstein, R. L. (2006) *Cell Metab.* **4**, 211–221
- Yamamoto, N., Ikeda, H., Tandon, N. N., Herman, J., Tomiyama, Y., Mitani, T., Sekiguchi, S., Lipsky, R., Kralisz, U., and Jamieson, G. A. (1990) *Blood* **76**, 1698–1703
- Curtis, B. R., and Aster, R. H. (1996) *Transfusion* **36**, 331–334
- Nozaki, S., Kashiwagi, H., Yamashita, S., Nakagawa, T., Kostner, B., Tomiyama, Y., Nakata, A., Ishigami, M., Miyagawa, J., and Kameda-Takemura, K. (1995) *J. Clin. Invest.* **96**, 1859–1865
- Janabi, M., Yamashita, S., Hirano, K., Sakai, N., Hiraoka, H., Matsumoto, K., Zhang, Z., Nozaki, S., and Matsuzawa, Y. (2000) *Arterioscler. Thromb. Vasc. Biol.* **20**, 1953–1960
- Moore, K. J., and Freeman, M. W. (2006) *Arterioscler. Thromb. Vasc. Biol.* **26**, 1702–1711
- Silverstein, R. L., and Febbraio, M. (2009) *Sci. Signal.* **2**, re3
- Ghosh, A., Li, W., Febbraio, M., Espinola, R. G., McCrae, K. R., Cockrell, E., and Silverstein, R. L. (2008) *J. Clin. Invest.* **118**, 1934–1943
- Bustelo, X. R. (2001) *Oncogene* **20**, 6372–6381
- Swat, W., and Fujikawa, K. (2005) *Immunol. Res.* **32**, 259–265
- Graham, D. B., Robertson, C. M., Bautista, J., Mascarenhas, F., Diacovo, M. J., Montgrain, V., Lam, S. K., Cremasco, V., Dunne, W. M., Faccio, R., Coopersmith, C. M., and Swat, W. (2007) *J. Clin. Invest.* **117**, 3445–3452
- Miletic, A. V., Graham, D. B., Montgrain, V., Fujikawa, K., Kloepfel, T., Brim, K., Weaver, B., Schreiber, R., Xavier, R., and Swat, W. (2007) *Blood* **109**, 3360–3368
- Wilkinson, B., Koenigsnecht-Talboo, J., Grommes, C., Lee, C. Y., and Landreth, G. (2006) *J. Biol. Chem.* **281**, 20842–20850
- Malhotra, S., Kovats, S., Zhang, W., and Coggeshall, K. M. (2009) *J. Biol. Chem.* **284**, 24088–24097
- Turner, M., and Billadeau, D. D. (2002) *Nat. Rev. Immunol.* **2**, 476–486
- Wells, C. M., Bhavsar, P. J., Evans, I. R., Vigorito, E., Turner, M., Tybulewicz, V., and Ridley, A. J. (2005) *Exp. Cell Res.* **310**, 303–310
- Pearce, A. C., Senis, Y. A., Billadeau, D. D., Turner, M., Watson, S. P., and Vigorito, E. (2004) *J. Biol. Chem.* **279**, 53955–53962
- Li, A. C., Binder, C. J., Gutierrez, A., Brown, K. K., Plotkin, C. R., Pattison, J. W., Valledor, A. F., Davis, R. A., Willson, T. M., Witztum, J. L., Palinski, W., and Glass, C. K. (2004) *J. Clin. Invest.* **114**, 1564–1576
- Harb, D., Bujold, K., Febbraio, M., Sirois, M. G., Ong, H., and Marleau, S. (2009) *Cardiovasc. Res.* **83**, 42–51
- Park, Y. M., Febbraio, M., and Silverstein, R. L. (2009) *J. Clin. Invest.* **119**, 136–145
- Moore, K. J., Kunjathoor, V. V., Koehn, S. L., Manning, J. J., Tseng, A. A., Silver, J. M., McKee, M., and Freeman, M. W. (2005) *J. Clin. Invest.* **115**, 2192–2201
- Kennedy, D. J., Kuchibhotla, S. D., Guy, E., Park, Y. M., Nimako, G., Vanegas, D., Morton, R. E., and Febbraio, M. (2009) *Arterioscler. Thromb. Vasc. Biol.* **29**, 1481–1487
- Marleau, S., Harb, D., Bujold, K., Avallone, R., Iken, K., Wang, Y., Demers, A., Sirois, M. G., Febbraio, M., Silverstein, R. L., Tremblay, A., and Ong, H. (2005) *FASEB J.* **19**, 1869–1871
- Knowles, J. W., Wang, H., Itakura, H., Southwick, A., Myers, R. M., Iribarren, C., Fortmann, S. P., Go, A. S., Quertermous, T., and Hlatky, M. A. (2007) *Am. Heart J.* **154**, 1052–1058
- Benton, R., Vannice, K. S., and Voshall, L. B. (2007) *Nature* **450**, 289–293
- Stuart, L. M., Deng, J., Silver, J. M., Takahashi, K., Tseng, A. A., Hennessy, E. J., Ezekowitz, R. A., and Moore, K. J. (2005) *J. Cell Biol.* **170**, 477–485